Catalysis Science & Technology

Accepted Manuscript

ROYAL SOCIETY OF CHEMISTRY

www.rsc.org/catalysis

Draft of April 16, 2014
prepared for *Catalysis Sci. Tech.*

Mechanistic Analysis of Water Oxidation Catalyzed by Mononuclear Copper in Aqueous Bicarbonate Solutions

Stuart G. Winikoff and Christopher J. Cramer*

Department of Chemistry, Chemical Theory Center, and Supercomputing Institute, 207 Pleasant St. SE, Minneapolis, MN 55455, USA.

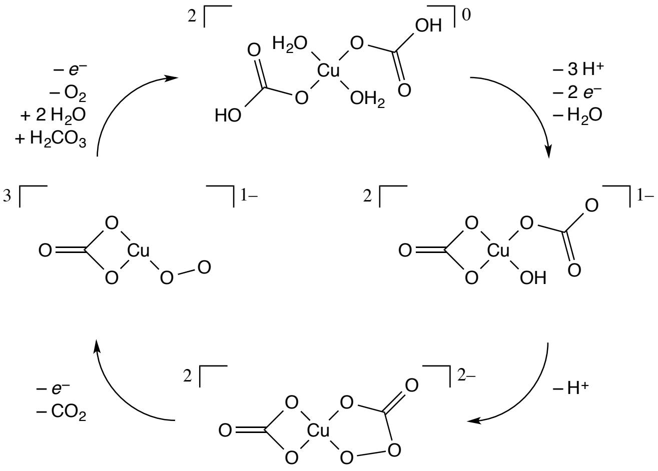

Abstract. We characterize a mechanism for a monomeric copper catalyst reported to oxidize water in bicarbonate solution when subject to sufficiently high external potentials at near neutral pH values. Density functional computations establish the thermochemical equilibria associated with microscopic redox and proton transfer steps and further reveal that O–O bond formation is associated with the unusual reaction of a coordinated hydroxide and carbonate ligand to generate a peroxycarbonate intermediate. The peroxycarbonate complex then decomposes through a retrocyclization to liberate O_2 and CO_2 and ultimately complete the catalytic cycle.

Keywords. Energy, Homogeneous catalysis, Water splitting, Reduction potential, Oxygen generation.

*cramer@umn.edu

Broader Context. Water oxidation is a reaction the study of which has seen an explosive growth in activity in the last several years, driven primarily by the desire to generate alternative fuels derived from green sources. Early work with relatively rare transition-metal based catalysts has generated a number of fundamental insights with respect to the range of possible catalytic activities and mechanisms, while more recent work has focused on the design of catalytic systems based on less costly earth-abundant metals, e.g., copper, iron, or cobalt, with an ultimate goal of improving economic viability. Importantly, while catalytic activities have been identified by experiment in several interesting systems, mechanistic details have been slower to emerge (although experimental data impose limits on mechanistic possibilities). With newly developed tools, including robust density functional models capable of handling metals in multiple, and sometimes unusual, oxidation states, as well as models that can treat often decisive solvation effects associated with aqueous ligands and first solvation shells, chemical theory offers an opportunity to elucidate mechanisms in order to facilitate next-generation design efforts by highlighting those factors that contribute to catalytic activity and efficiency.

Production of hydrogen gas from the oxidation of water generates a green fuel, potentially through the exploitation green sources of oxidizing power, and this process is now the subject of considerable research activity.[1-9] Many transition-metal-based homogeneous catalysts for water oxidation have been reported, especially those incorporating Ir[10-14] and Ru.[15-29] Reports of homogeneous catalysts based on more earth-abundant metals,[30-32] e.g., Mn,[33-36] Co,[37-51] Fe,[52-57] and Cu,[58-61] have also recently begun to appear. High turn-over frequencies have been reported for several copper-based catalysts active predominantly at high pH and high potential, but detailed mechanisms for the observed oxidation of water in these systems have not yet been established.

In this work, we use density functional theory[62-64] (DFT) in conjunction with micro- and implicit solvation models[63,65,66] (SMD/M11-L/SDD|6-311+G(d,p), see supporting information for full computational details) to analyze mechanistic pathways for the production of molecular oxygen from mononuclear Cu^{II} complexes reported to be active in aqueous bicarbonate/CO_2 solutions over the pH range 6.7-8.2.[59] We identify a thermochemically accessible cycle for oxidation of the catalyst that leads to O–O bond formation and O_2 release with all steps consistent with reported experimental observations, such comparisons being key to validation of the theoretical model.

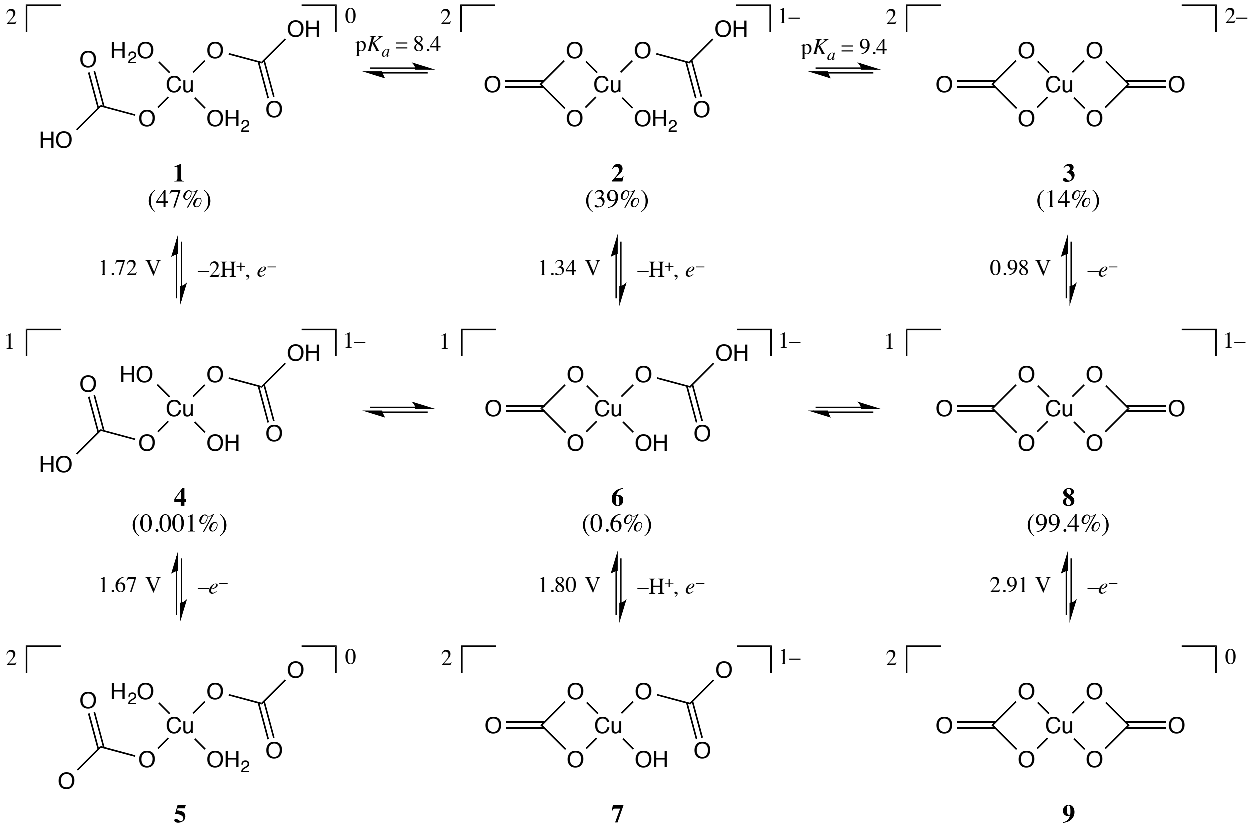

Figure 1. Compounds relevant to initial oxidation steps in copper-bicarbonate catalyzed water splitting. Voltages vs the standard hydrogen electrode (SHE) are provided for elementary steps at pH = 8.2. Percentages of contributors to equilibrium populations (top and middle rows) are also reported for pH = 8.2. Charges and spin multiplicities for all species are indicated at upper right and upper left of structures, respectively.

Theory predicts a conjugate acid/base speciation of Cu^{II} compounds dominated by bis-monodentate bicarbonate species below a pH of 8.4, mixed mono- and bidentate bicarbonate and carbonate, respectively, between a pH of 8.4 and 9.4, and bis bidentate carbonate above pH 9.4 (Figure 1). This prediction is in fairly good energetic agreement with electron spin-echo envelope modulation experiments that found analogous 14 K frozen solutions of copper in aqueous bicarbonate at pH values of 5.5, 6.5, and 8.0 to exhibit all monodentate, some bidentate, and bis bidentate anion coordination, respectively.[67] Given the uncertainties associated with comparing frozen and liquid samples, we consider this agreement to contribute acceptably to validation of the computational protocol for acid/base speciation in related compounds.

We next consider the standard reduction potentials associated with possible oxidations of the various conjugate acid and base forms present in solution at the experimental pH of 8.2 (Figure 1). The most facile oxidation is predicted to be oxidation of **3** by one electron to give **8**. The predicted potential (which is pH independent for this case as only electron transfer is involved) is 0.98 V. This agrees well with an onset potential of 1.05 V measured by cyclic voltammetry at a higher pH of 10.8,[59] at which pH compound **3** would be expected to be the dominant reduced species in solution. We predict compound **8** to be in equilibrium at pH = 8.2 with conjugate acid forms **4** and **6**, which replace bidentate carbonate coordination with monodentate bicarbonate coordination and hydroxide ligands (formal oxidation potentials for proton-coupled electron transfer processes generating **4** and **6** from **1** and **2** are shown in Figure 1 for completeness). Further oxidation of **6** and **8** is not predicted to occur for potentials below 1.8 V, but **4** is predicted to be subject to additional 1-electron oxidation with tautomerization to a diaquocopper species **5** at a potential of 1.67 V, which is very close to the applied potential of 1.65 V at which experimental catalysis is observed.[59] Thus, while the equilibrium of **4**, **6**, and **8** is predicted to be dominated by **8** (99.4%), further oxidation chemistry is predicted to drain that equilibrium through oxidation of minor component **4**. The resulting product compound **5** is predicted to have substantial unpaired spin density on the two formal carbonate ligands, indicating that a full Cu^{IV} oxidation state is not achieved in **5**.

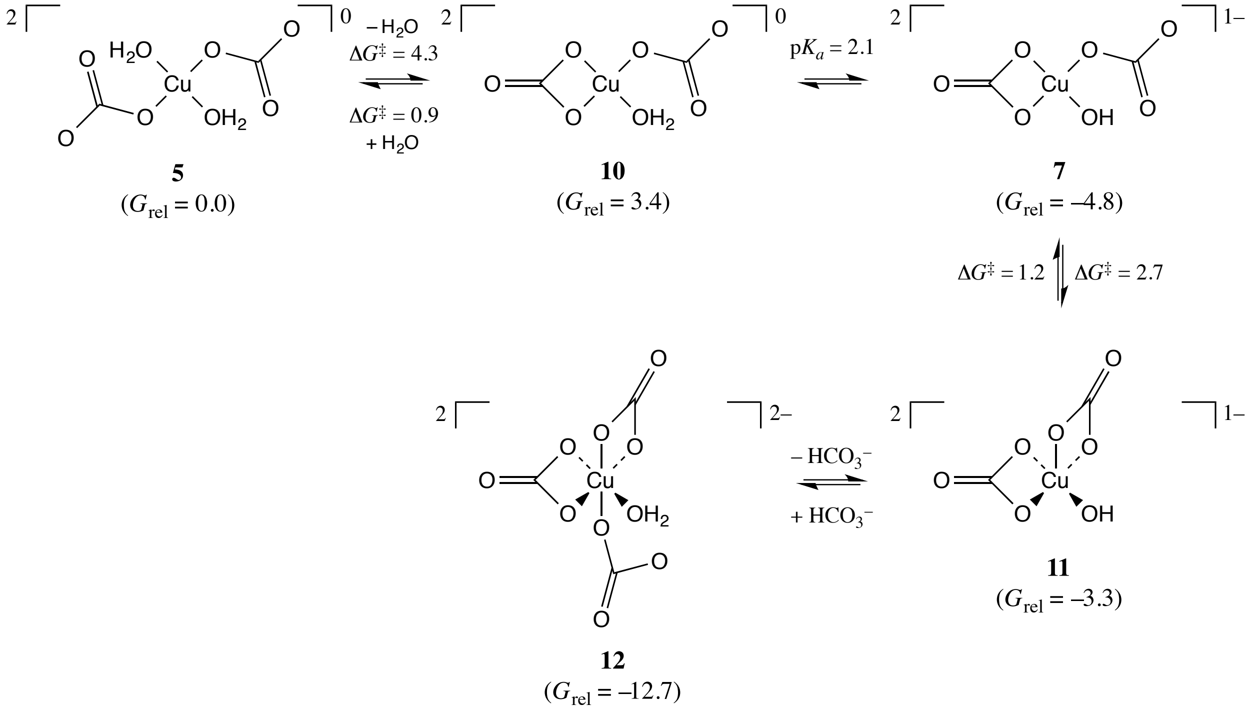

Figure 2. Conformers and conjugate acid/base forms for 2-electron oxidized intermediates relevant to the catalytic cycle. Relative free energies (kcal mol^{-1}) at pH 8.2 and 1 M bicarbonate are shown taking **5** as the zero of energy. Free energies of activation are reported for individual microscopic steps. Charges and spin multiplicities for all species are indicated at upper right and upper left of structures, respectively.

Chemical steps permit the conversion of **5** to species **7** as shown in Figure 2. With an activation free energy of 4.3 kcal mol^{-1} , one carbonate unit displaces an aquo ligand to become bidentate, and the resulting intermediate **10** is predicted to be unstable to loss of a proton to provide **7** which is 4.8 kcal mol^{-1} lower in energy than **5** at pH = 8.2. Compound **7** itself is in equilibrium with its conformational isomer **11**, in which the second carbonate ligand is also bidentate, with **11** being 1.5 kcal mol^{-1} higher in energy than **7**. Coordination of an additional bicarbonate ligand in a monodentate fashion, generates structure **12**, stabilized by hydrogen bonding to a non-coordinated carbonate oxygen atom after proton transfer to form an aquo ligand. At the experimental bicarbonate concentration of 1 M, **12** is predicted to be the thermodynamic sink for these various coordination compounds and a true, octahedral, Cu^{IV} species.

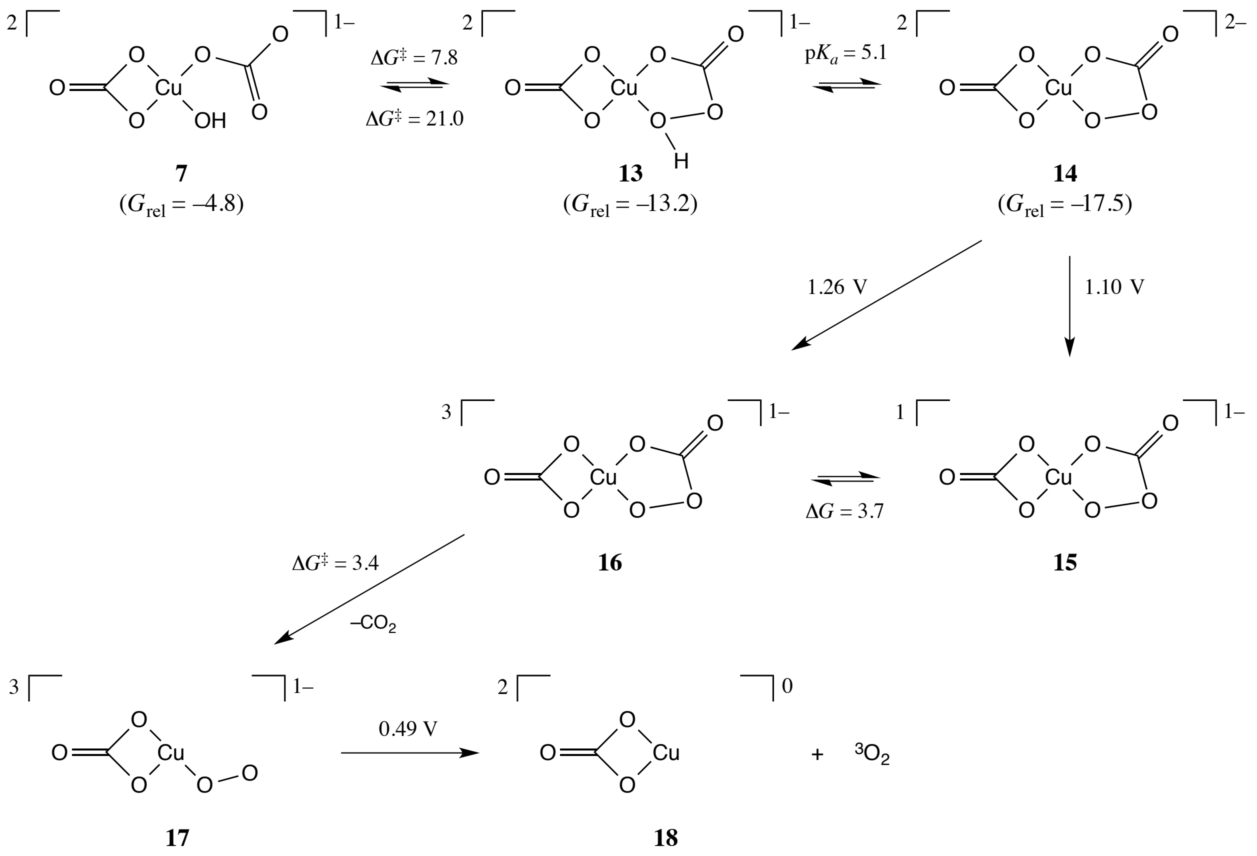

Figure 3. Final steps relevant to the catalytic cycle. For the top row of species, relative free energies (kcal mol^{-1}) at pH 8.2 are shown taking **5** as the zero of energy. Free energies of activation are reported for individual microscopic steps. Voltages vs the standard hydrogen electrode (SHE) are provided for elementary steps. Charges and spin multiplicities for all species are indicated at upper right and upper left of structures, respectively.

While **12** prevails at equilibrium, we found no viable reaction paths for the generation of an O–O bond through reactions of the ligands of **12**, whether with one another or with solvent water (details for several unproductive pathways are provided in full in the supporting information). However, as shown in Figure 3, O–O bond formation *is* predicted to take place in **7**, and involves reaction between the hydroxide ligand and one of the uncoordinated carbonate oxygen atoms with an activation free energy of 7.8 kcal mol^{-1} (which is 15.7 kcal mol^{-1} relative to **12**; transition-state (TS) structure in Figure 4). The forming O–O bond length in the TS structure is predicted to be 1.808 Å. The resulting peroxybicarbonate compound **13**, which is predicted to be 0.5 kcal mol^{-1} *lower* in energy than **12**, is predicted to deprotonate spontaneously at pH = 8.2 to generate **14**.

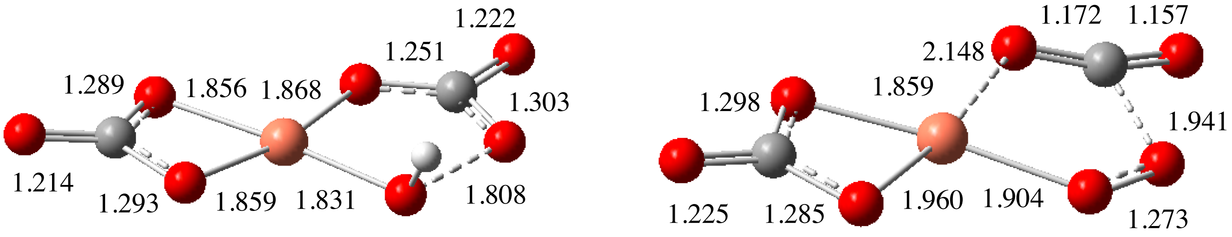

Figure 4. Optimized TS structures for O–O bond formation (left) and CO_2 loss (right) with heavy-atom bond lengths (Å). Atom colors are white (hydrogen), gray (carbon), red (oxygen) and apricot (copper).

Compound **14** is predicted to undergo 1-electron oxidation at a potential of 1.10 V. The resulting formal Cu^{III} species **15** has a singlet ground state, but its corresponding triplet excited state **16** is predicted to be only 3.7 kcal mol^{-1} higher in energy (and indeed, this implies oxidation of doublet **14** may access **16** directly with applied potentials in excess of 1.26 V). The triplet state is important because it is on the triplet surface that a retrocyclization reaction is found to occur with a very low activation free energy of 3.4 kcal mol^{-1} to liberate CO_2 and generate copper superoxo species **17** (TS structure in Figure 4). Loss of CO_2 is predicted to be exergonic by 6.7 kcal mol^{-1}. The TS structure for the retrocyclization has breaking Cu–O and C–O bond distances of 2.148 and 1.941 Å, respectively, and the forming carbon dioxide fragment already has C=O bonds shorter than 1.2 Å. Another interesting feature of the TS structure is that the O_2

fragment appears to be only relatively weakly interacting with the Cu atom; it has a quite short O–O bond length of 1.273 Å and relatively long Cu–O bond of 1.904 Å.

It is noteworthy that while spin-orbit coupling would be expected to permit **15** and **16** to equilibrate, it may be sufficiently slow that modest concentrations of singlet **15** can be present under catalytic conditions. This may explain the experimental observation of a re-reduction wave at about 1.25 V for scan rates in excess of 500 mV/s. The good agreement in the observed and predicted potentials for this process may be taken as a further validation of the computational model.

Once generated, triplet Cu^{II} superoxo species **17** is susceptible to one-electron oxidation with a predicted standard potential of 0.49 V. Upon oxidation, the Cu–O bond to the O_2 fragment spontaneously breaks, and full dissociation of molecular oxygen from the copper carbonate compound **18** is predicted to be exergonic by 6.5 kcal mol^{-1}. To complete the catalytic cycle, **18** simply coordinates two water molecules and one carbonic acid molecule (which may be regarded as having been generated by loss of one water and one CO_2 during intermediate steps in the catalytic cycle).

Conclusions

This copper-based catalytic process is particularly interesting in so far as CO_2 effectively serves as a co-catalyst, activating one water molecule to participate in the O–O bond forming step by first reacting with it to generate carbonic acid, and then coordinating in a conjugate base form to the metal center to act as a (non-innocent and reactive) ligand during a portion of the catalytic cycle. Beyond the co-catalysis, CO_2 also buffers the solution to more neutral pH values where overpotentials associated with working against a large proton concentration may be associated with proton-coupled electron-transfer steps.

Key factors contributing to the catalytic efficiency of this system are (i) the small energy differences associated with monodentate vs. bidentate coordination motifs for bicarbonate and carbonate ligands, which facilitates ligand shuffling in order to organize a pre-O–O bond forming complex, (ii) the degree to which the carbonate and peroxycarbonate ligands are able to delocalize spin density through Cu–O covalency, thereby facilitating an unusual electrophilic O–O bond formation between a hydroxyl ligand and a carbonate ligand, and (iii) the small singlet-triplet splitting in the bidentate peroxycarbonate complex **15**/**16**, which is again associated with the propensity of the ligands to be non-innocent, and facilitates retrocyclic CO_2 elimination on the triplet surface. The low predicted free energy of activation for the O–O bond forming step, 15.7 kcal mol^{-1} relative to its lowest energy equilibrium precursor, is particularly noteworthy in so far as most other water oxidation catalysts for which activation free energies for this step have been reported tend to be characterized by values closer to 20 kcal mol^{-1}.

We close by nothing that the efficiency of the catalytic system reported by Chen and Meyer[59] *increases* at pH values above 8.2, but analysis of the relevant reaction kinetics indicates that water oxidation becomes *second*-order in copper under these conditions. Characterizing the ability of dicopper systems to make and break O–O bonds has been a particularly active area of research,[68-72] and it will be fascinating to see the degree to which prior work on oxygen activation will connect with observed water oxidation in aqueous carbonate solutions.

Supporting Information. Full details for theoretical methods, characterization of uncompetitive alternative pathways for catalysis, and Cartesian coordinates for all structures.

Acknowledgments. This research was supported by a grant from the U.S. National Science Foundation (CHE-0952054).

Notes and References

1. L. L. Tinker, N. D. McDaniel and S. Bernhard, *J. Mater. Chem.*, 2009, **19**, 3328.
2. H. Dau, C. Limberg, T. Reier, M. Risch, S. Roggan and P. Strasser, *Chemcatchem*, 2010, **2**, 724.
3. H. Yamazaki, A. Shouji, M. Kajita and M. Yagi, *Coord. Chem. Rev.*, 2010, **254**, 2483.
4. A. Llobet and F. Meyer, *Angew. Chem. Int. Ed.*, 2011, **50**, A30.
5. S. Fukuzumi, T. Kishi, H. Kotani, Y.-M. Lee and W. Nam, *Nat Chem*, 2011, **3**, 38.

6. C. Herrero, A. Quaranta, W. Leibl, A. W. Rutherford and A. Aukauloo, *Energy Environ. Sci.*, 2011, **4**, 2353.
7. D. Gust, T. A. Moore and A. L. Moore, *Faraday Discuss.*, 2012, **155**, 9.
8. K. S. Joya, J. L. Valles-Pardo, Y. F. Joya, T. Eisenmayer, B. Thomas, F. Buda and H. J. M. de Groot, *Chempluschem*, 2013, **78**, 35.
9. J. R. Swierk and T. E. Mallouk, *Chem. Soc. Rev.*, 2013, **42**, 2357.
10. N. D. McDaniel, F. J. Coughlin, L. L. Tinker and S. Bernhard, *J. Am. Chem. Soc.*, 2007, **130**, 210.
11. J. D. Blakemore, N. D. Schley, D. Balcells, J. F. Hull, G. W. Olack, C. D. Incarvito, O. Eisenstein, G. W. Brudvig and R. H. Crabtree, *J. Am. Chem. Soc.*, 2010, **132**, 16017.
12. L. Vilella, P. Vidossich, D. Balcells and A. Lledos, *Dalton Trans.*, 2011, **40**, 11241.
13. D. C. Hong, M. Murakami, Y. Yamada and S. Fukuzumi, *Energy Environ. Sci.*, 2012, **5**, 5708.
14. J. DePasquale, I. Nieto, L. E. Reuther, C. J. Herbst-Gervasoni, J. J. Paul, V. Mochalin, M. Zeller, C. M. Thomas, A. W. Addison and E. T. Papish, *Inorg. Chem.*, 2013, **52**, 9175.
15. S. W. Gersten, G. J. Samuels and T. J. Meyer, *J. Am. Chem. Soc.*, 1982, **104**, 4029.
16. X. Yang and M. H. Baik, *J. Am. Chem. Soc.*, 2008, **130**, 16231.
17. F. Bozoglian, S. Romain, M. Z. Ertem, T. K. Todorova, C. Sens, J. Mola, M. Rodriguez, I. Romero, J. Benet-Buchholz, X. Fontrodona, C. J. Cramer, L. Gagliardi and A. Llobet, *J. Am. Chem. Soc.*, 2009, **131**, 15176.
18. X. Sala, I. Romero, M. Rodriguez, L. Escriche and A. Llobet, *Angew. Chem. Int. Ed.*, 2009, **48**, 2842.
19. D. J. Wasylenko, C. Ganesamoorthy, M. A. Henderson, B. D. Koivisto, H. D. Osthoff and C. P. Berlinguette, *J. Am. Chem. Soc.*, 2010, **132**, 16094.
20. X. C. Li, G. J. Chen, S. Schinzel and P. E. M. Siegbahn, *Dalton Trans.*, 2011, **40**, 11296.
21. S. Ghosh and M. H. Baik, *Inorg. Chem.*, 2011, **50**, 5946.
22. L. L. Duan, C. M. Araujo, M. S. G. Ahlquist and L. C. Sun, *Proc. Natl. Acad. Sci., USA*, 2012, **109**, 15584.
23. T. Wada, H. Ohtsu and K. Tanaka, *Chem. Eur. J.*, 2012, **18**, 2374.
24. N. Kaveevivitchai, R. F. Zong, H. W. Tseng, R. Chitta and R. P. Thummel, *Inorg. Chem.*, 2012, **51**, 2930.
25. S. Ghosh and M.-H. Baik, *Angew. Chem. Int. Ed.*, 2012, **51**, 1221.
26. A. Kimoto, K. Yamauchi, M. Yoshida, S. Masaoka and K. Sakai, *Chem. Commun.*, 2012, **48**, 239.
27. R. Kang, J. Yao and H. Chen, *J. Chem. Theory Comput.*, 2013, **9**, 1872.
28. M. Hirahara, M. Z. Ertem, M. Komi, H. Yamazaki, C. J. Cramer and M. Yagi, *Inorg. Chem.*, 2013, **52**, 6354.
29. L. Vaquer, P. Miro, X. Sala, F. Bozoglian, E. Masllorens, J. Benet-Buchholz, X. Fontrodona, T. Parella, I. Romero, A. Roglans, M. Rodriguez, C. Bo and A. Llobet, *Chempluschem*, 2013, **78**, 235.
30. J. M. Saveant, *Chem. Rev.*, 2008, **108**, 2348.
31. R. Cao, W. Z. Lai and P. W. Du, *Energy Environ. Sci.*, 2012, **5**, 8134.
32. A. Singh and L. Spiccia, *Coord. Chem. Rev.*, 2013, **257**, 2607.
33. C. W. Cady, R. H. Crabtree and G. W. Brudvig, *Coord. Chem. Rev.*, 2008, **252**, 444.
34. C. Herrero, A. Quaranta, S. Protti, W. Leibl, A. W. Rutherford, R. Fallahpour, M. F. Charlot and A. Aukauloo, *Chem. Asian J.*, 2011, **6**, 1335.

35. E. A. Karlsson, B. L. Lee, T. Akermark, E. V. Johnston, M. D. Karkas, J. L. Sun, O. Hansson, J. E. Backvall and B. Akermark, *Angew. Chem. Int. Ed.*, 2011, **50**, 11715.
36. P. E. M. Siegbahn and M. R. A. Blomberg, *J. Chem. Theory Comput.*, 2014, **10**, 268.
37. Q. Yin, J. M. Tan, C. Besson, Y. V. Geletii, D. G. Musaev, A. E. Kuznetsov, Z. Luo, K. I. Hardcastle and C. L. Hill, *Science*, 2010, **328**, 342.
38. V. Artero, M. Chavarot-Kerlidou and M. Fontecave, *Angew. Chem. Int. Ed.*, 2011, **50**, 7238.
39. D. K. Dogutan, R. McGuire and D. G. Nocera, *J. Am. Chem. Soc.*, 2011, **133**, 9178.
40. J. B. Gerken, J. G. McAlpin, J. Y. C. Chen, M. L. Rigsby, W. H. Casey, R. D. Britt and S. S. Stahl, *J. Am. Chem. Soc.*, 2011, **133**, 14431.
41. L. P. Wang and T. Van Voorhis, *J. Phys. Chem. Lett.*, 2011, **2**, 2200.
42. D. J. Wasylenko, C. Ganesamoorthy, J. Borau-Garcia and C. P. Berlinguette, *Chem. Commun.*, 2011, **47**, 4249.
43. M. L. Rigsby, S. Mandal, W. Nam, L. C. Spencer, A. Llobet and S. S. Stahl, *Chem. Sci.*, 2012, **3**, 3058.
44. M. Z. Ertem and C. J. Cramer, *Dalton Trans.*, 2012, **41**, 12213.
45. S. Goberna-Ferron, L. Vigara, J. Soriano-Lopez and J. R. Galan-Mascaros, *Inorg. Chem.*, 2012, **51**, 11707.
46. D. Hong, J. Jung, J. Park, Y. Yamada, T. Suenobu, Y. M. Lee, W. Nam and S. Fukuzumi, *Energy Environ. Sci.*, 2012, **5**, 7606.
47. G. La Ganga, F. Puntoriero, S. Campagna, I. Bazzan, S. Berardi, M. Bonchio, A. Sartorel, M. Natali and F. Scandola, *Faraday Discuss.*, 2012, **155**, 177.
48. E. Pizzolato, M. Natali, B. Posocco, A. M. Lopez, I. Bazzan, M. Di Valentin, P. Galloni, V. Conte, M. Bonchio, F. Scandola and A. Sartorel, *Chem. Commun.*, 2013, **49**, 9941.
49. X. Li and P. E. M. Siegbahn, *J. Am. Chem. Soc.*, 2013.
50. K. Kwapien, S. Piccinin and S. Fabris, *J. Phys. Chem. Lett.*, 2013, **4**, 4223.
51. H. T. Lei, A. Han, F. W. Li, M. N. Zhang, Y. Z. Han, P. W. Du, W. Z. Lai and R. Cao, *Phys. Chem. Chem. Phys.*, 2014, **16**, 1883.
52. W. C. Ellis, N. D. McDaniel, S. Bernhard and T. J. Collins, *J. Am. Chem. Soc.*, 2010, **132**, 10990.
53. J. L. Fillol, Z. Codolà, I. Garcia-Bosch, L. Gómez, J. J. Pla and M. Costas, *Nat Chem*, 2011, **3**, 807.
54. M. Z. Ertem, L. Gagliardi and C. J. Cramer, *Chem. Sci.*, 2012, **3**, 1293.
55. W. A. Hoffert, M. T. Mock, A. M. Appel and J. Y. Yang, *Eur. J. Inorg. Chem.*, 2013, **2013**, 3846.
56. D. Hong, S. Mandal, Y. Yamada, Y. M. Lee, W. Nam, A. Llobet and S. Fukuzumi, *Inorg. Chem.*, 2013, **52**, 9522.
57. R.-Z. Liao, X.-C. Li and P. E. M. Siegbahn, *Eur. J. Inorg. Chem.*, 2014, **2014**, 728.
58. S. M. Barnett, K. I. Goldberg and J. M. Mayer, *Nature Chemistry*, 2012, **4**, 498.
59. Z. Chen and T. J. Meyer, *Angew. Chem. Int. Ed.*, 2013, **52**, 700.
60. M.-T. Zhang, Z. Chen, P. Kang and T. J. Meyer, *J. Am. Chem. Soc.*, 2013, **135**, 2048.
61. T. Zhang, C. Wang, S. B. Liu, J. L. Wang and W. B. Lin, *J. Am. Chem. Soc.*, 2014, **136**, 273.
62. C. J. Cramer, *Essentials of Computational Chemistry: Theories and Models*, 2nd edn., John Wiley & Sons, Chichester, 2004.
63. C. J. Cramer and D. G. Truhlar, *Phys. Chem. Chem. Phys.*, 2009, **11**, 10757.

64. W. Koch and M. C. Holthausen, *A Chemist's Guide to Density Functional Theory*, 2nd edn., Wiley-VCH, Weinheim, 2011.
65. A. V. Marenich, C. J. Cramer and D. G. Truhlar, *J. Phys. Chem. B*, 2009, **113**, 6378.
66. A. V. Marenich, A. Majumdar, M. Lenz, C. J. Cramer and D. G. Truhlar, *Angew. Chem. Int. Ed.*, 2012, **51**, 12810.
67. P. M. Schosseler, B. Wehrli and A. Schweiger, *Inorg. Chem.*, 1997, **36**, 4490.
68. E. I. Solomon, U. M. Sundaram and T. E. Machonkin, *Chem. Rev.*, 1996, **96**, 2563.
69. P. E. M. Siegbahn, *J. Biol. Inorg. Chem.*, 2003, **8**, 577.
70. L. Q. Hatcher and K. D. Karlin, *J. Biol. Inorg. Chem.*, 2004, **9**, 669.
71. E. A. Lewis and W. B. Tolman, *Chem. Rev.*, 2004, **104**, 1047.
72. B. F. Gherman and C. J. Cramer, *Coord. Chem. Rev.*, 2009, **253**, 723.